Ab Initio Fermi Surface Calculation for Charge-Density Wave Instability in Transition Metal Oxide Bronzes

Eric Sandre, Pascale Foury-Leylekian, Sylvain Ravy, and Jean-Paul Pouget
Laboratoire de Physique des Solides (UMR 8502), Université Paris-Sud, Bâtiment 510, 91405 Orsay CEDEX, France
(Received 29 September 2000)

The electronic structure of the charge density wave (CDW) bronze $(PO_2)_4(WO_3)_{2m}$, $m = 4$, is determined using *ab initio* density functional theory. The calculation shows that the Fermi surface (FS) consists in the superposition of three one-dimensional FS's associated with three types of chains. The q dependence of the electronic response function calculated from the electronic structure quantitatively accounts for the anisotropy of the fluctuations probed by x-ray diffuse scattering. The results validate the hidden nesting mechanism proposed for the CDW transitions in this series of bronzes.

DOI: 10.1103/PhysRevLett.86.5100 PACS numbers: 71.45.Lr, 71.18.+y, 64.60.–i, 71.20.Mq

Because they exhibit a large variety of macroscopic quantum phenomena such as superconductivity, charge density wave (CDW), and spin density waves, low-dimensional metals are extensively studied [1]. The understanding of these phenomena requires nontrivial calculations of the electronic response, including the effect of electron-electron correlation and coupling of the conduction electrons with the lattice degrees of freedom. The layered transition metal oxide bronzes belong to these classes of metals. Superconductivity has been discovered in the A_xWO_3 (A = Na and Rb) and WO_{3-x} tungsten bronzes, in the molybdenum purple bronze $Li_{0.9}Mo_6O_{17}$, and very recently, CDW instabilities were observed in other Mo and W bronzes [2,3]. The general formula of bronzes is $A_x(M_yO_z)$ where A is a cation or an elemental group and M_yO_z a transition metal (M) oxide. The presence of A_x induces a partial filling of the bands formed by the transition metal d t_{2g}-orbitals. The bronzes provide a natural class of low-dimensional materials because of the directed character of the d orbitals which induces bonding anisotropy. Based on MO_6 octahedral basic units, the structures observed can be one, two, or three dimensional (1D, 2D, or 3D) with respect to the chemical bond network but are 1D or 2D with respect to the anisotropy in the conductivity. The 2D case is particularly illustrated by the Mo purple bronzes $A_xMo_6O_{17}$ (A = K, Rb, Tl), the oxide Mo_4O_{11}, and the monophosphate tungsten bronzes with pentagonal tunnels (MPTBp's), $(PO_2)_4(WO_3)_{2m}$ ($4 \leq m \leq 14$). Mo_4O_{11} is isostructural to the $m = 6$ member of the MPTBp's. In all these compounds, the structure is made out of ReO_3-type corner-sharing MO_6 octahedra slabs, separated by either MoO_4 (in the case of $A_xMo_6O_{17}$ and Mo_4O_{11}) or PO_4 (in the MPTB bronzes) tetrahedra slabs. Surprisingly, first band structure calculations based on the extended Hückel semiempirical method [4,5] suggest that the conduction bands of these compounds are in fact the superposition of three separated 1D conduction bands which are built on different sets of t_{2g} orbitals. Each band corresponds to a 2D lattice of parallel infinite and weakly coupled chains of WO_6 octahedra running in different directions of the ReO_3-type slab. This implies that the Fermi surface (FS) can be decomposed into three underlying quasi-1D FS's, each of them being associated with one set of chains. Recent angle-resolved photoemission spectroscopy imaging of the FS of the purple bronzes [6] and of Mo_4O_{11} [7] support this interpretation.

All these 2D oxide bronzes exhibit one or several successive CDW transitions of the Peierls type [8]. The CDW state corresponds to a $2k_F$ modulation of the electronic density associated with a $2k_F$ periodic lattice distortion (PLD). In the 2D oxide bronzes, the Peierls transition, however, leads to the formation of a semimetallic state with small electron and hole pockets left after the incomplete FS nesting process [9]. This CDW ground state exhibits particularly interesting phenomena. For example, superconductivity has been found below 0.3 K in the $m = 7$ member of the MPTBp's [10] and Mo_4O_{11} exhibits a bulk quantum Hall effect [11].

The explanation of all these instabilities requires a detailed examination of the electronic structure of these oxide bronzes. No *ab initio* calculation had been performed so far because of a too large number of atoms per unit cell in these compounds. In this Letter, we present the first determination of the self-consistent electronic structure using the density functional theory (DFT) of the bronze with the smallest unit cell: the $m = 4$ member of the MPTBp's ($P_4W_8O_{32}$).

$P_4W_8O_{32}$ crystallizes in the $P2_12_12_1$ orthorhombic space group ($a = 0.5285$ nm, $b = 0.6569$ nm, and $c = 1.7351$ nm) [12]. The successive ab ReO_3-type slabs are related by screw axis symmetry along c. Each ab slab is made of segments of $m = 4$ corner-sharing WO_6 octahedra which terminate with PO_4 tetrahedra (see Fig. 6b in Ref. [12]). These segments are linked in a staircase manner, forming infinite ribbons (i.e., chains of octahedra) running in the $a \pm b$ symmetry related directions, and in the a direction. Empty pentagonal tunnels are created at the junction between the ReO_3-type slabs and the PO_4

 0031-9007/01/86(22)/5100(4)$15.00

tetrahedra. As each PO_2 group donates one electron, there is a density of four conduction electrons per unit cell. The $m = 4$ member shows clear anisotropic metallic transport properties with the electrical conductivity at least 1 order of magnitude higher in the ab plane than perpendicularly. The electrical conductivity exhibits also two giant anomalies around 80 K (Tc_1) and 52 K (Tc_2) which have been attributed to CDW transitions [9,13]. Indeed, crystallographic studies clearly demonstrate that each anomaly corresponds to the establishment of a long range incommensurate PLD with the modulation wave vectors $q_1 = [0.330(5), 0.295(5), 0]$ and $q_2 = [0.340(5), 0, 0]$, respectively [8,14].

X-ray diffuse scattering experiments show that the pretransitional fluctuations of these PLD give rise to modulated diffuse lines perpendicular to the a direction, and to broader diffuse lines perpendicular to $a \pm b$ (Fig. 1A). These diffuse lines, which can be detected up to room temperature, are due to the intersection of the Ewald sphere with diffuse sheets in reciprocal space. Such diffuse sheets correspond to the scattering by 1D lattice modulations [15]. These three directions are actually the ones along which run the infinite chains of WO_6 octahedra. Figure 1B gives a representation of the location of these diffuse sheets in the Brillouin zone. The position of the q_1 and q_2 satellite reflections stabilized below Tc_1 and Tc_2 is also indicated.

These diffuse sheets are the fingerprint of the electron gas instability toward the formation of a CDW [16,17]. Indeed, the CDW instability is coupled to the lattice (mostly the W atoms [14]) via the electron-phonon coupling. In the linear response theory, the relevant response of the electrons to a static modulation of the ionic position of wave vector q is given by the electron-hole Lindhard function [18,19]:

$$\chi(q,T) = -\sum_k \frac{\overline{n}_k - \overline{n}_{k+q}}{\varepsilon_k - \varepsilon_{k+q}}, \qquad (1)$$

where $\overline{n}_k$ ($\overline{n}_{k+q}$) is the Fermi-Dirac distribution associated with the electronic state with wave vector k ($k + q$) and the eigenenergy ε_k (ε_{k+q}). As is well known, the response function is significant when unoccupied states at the Fermi level are coupled by the wave vector q to occupied states of the same energy. This condition arises when the FS is composed of parts easily superimposed onto one another. These topological properties of the FS, called nesting properties, are perfectly obtained at $T = 0$ K for purely 1D metals when $q = 2k_F$ (k_F is the Fermi wave vector) [18]. The response function then presents a divergence leading to the so called CDW state. The simple 3D metals do not stabilize CDW states due to the absence of nesting properties of their FS. In 2D metals, the CDW stabilization depends on the particular topology of the FS. Because of the chainlike structure of their metallic layers, the bronzes exhibit an intermediate situation between the 1D and 2D cases. In the framework of the above quoted decomposition of the FS into quasi-1D FS's, the critical wave vector of the CDW instability q_i ($i = 1, 2$) could be stabilized by a hidden FS nesting mechanism which corresponds to a nesting of simultaneously several sets of differently oriented portions of quasi-1D FS [4].

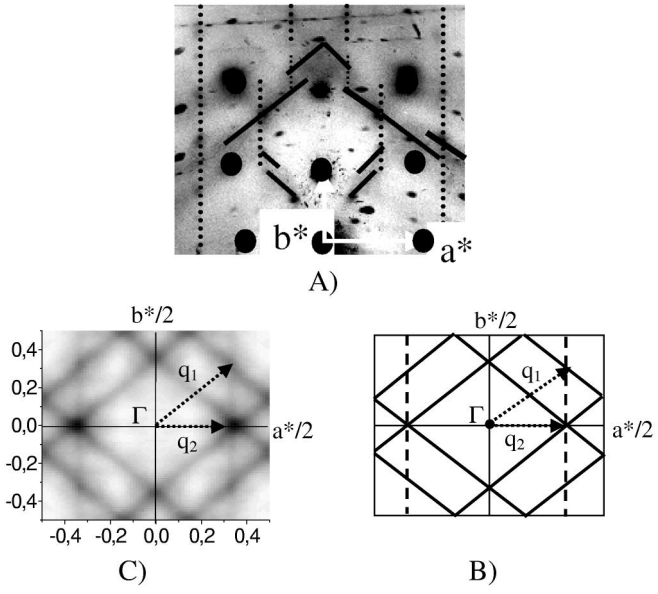

FIG. 1. $P_4W_8O_{32}$: (A) X-ray pattern taken at 300 K in the vicinity of the a^*b^* reciprocal plane. The critical diffuse scattering is marked by continuous (dashed) lines associated to the diffuse sheets perpendicular to the $a \pm b$ (a) directions. (B) Representation in the (a^*, b^*) section of the first Brillouin zone. The structure factor effects are neglected. The location of the diffuse lines, the q_1 and q_2 satellite reflections, and the Bragg reflections (dots) are represented. (C) DFT electron-hole response function at 100 K.

In order to calculate the response function of $P_4W_8O_{32}$, we have computed the electronic structure using the DFT. We have used a total energy scheme [20] based on ultrasoft pseudopotentials [21] with a plane-wave basis set cutoff energy of 400 eV. The exchange and correlation energy was calculated using the local density approximation. The sets of irreducible k points used in the Brillouin zone integration were generated according to the Monkhost-Pack scheme using a spacing of 0.5 nm^{-1} which was found to be sufficient to converge the total energy. The total energy was minimized using a conjugate gradient and density mixing scheme [22]. Once the total energy and electronic density were converged, we performed a series of eigenvalue calculations for both the occupied and 12 unoccupied eigenstates on a grid of 100 special k points scattered inside the ($c^* = 0$) reciprocal space plane. A subsequent interpolation of the different bands along the $a^* + (1/n)b^*$ (n integer) direction was then performed to determine the exact different k points for which the eigenenergies equal the Fermi energy which was previously estimated during the self-consistent run.

The calculated band structure presented in Fig. 2 shows that the energy dispersion is 100 times smaller along the c^* direction than along the a^* and b^* ones, which confirms

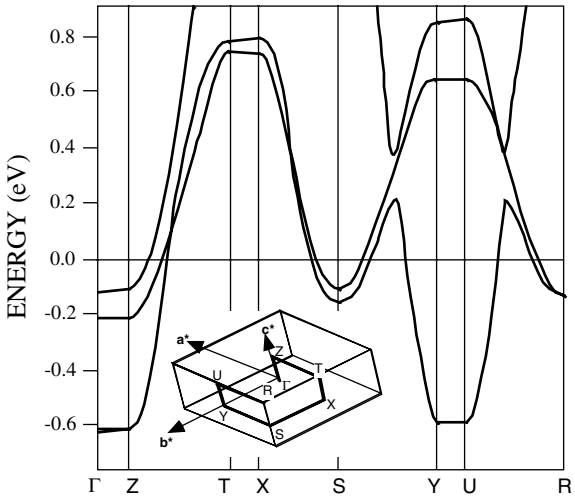

FIG. 2. Band dispersion of $P_4W_8O_{32}$ along several symmetry directions of the Brillouin zone indicated in the inset.

the 2D character of the compound. The average Fermi energy (E_F) is found to be $1/3$ eV, which is in agreement with the value extracted from the thermal dependence of the thermopower [23]. Furthermore, recent photoemission measurements [24] for the three bands lead to E_F values close to that obtained in Fig. 2. We can notice that although the band structure calculated here is similar to the one obtained using the extended Hückel approximation [25], the Fermi energies obtained are different. The extended Hückel method gives a value 3 times smaller. It is experimentally found that the extended Hückel calculations always underestimate the bandwidth in the bronzes [26].

As there is no significant dispersion along the c^* axis, we have restrained the FS surface calculation to the a^*b^* reciprocal plane of the Brillouin zone. A plot of the obtained FS is shown in Fig. 3 (the double lines are due to the splitting of the single layer bands by the interlayer coupling). The dashed lines give a schematic representation of this FS. This schematical ideal FS can be considered as the superimposition of three 1D FS's, each corresponding to the three almost noncorrelated WO_6 chains inside the ab plane. The self-consistent DFT calculation comforts the hidden nesting hypothesis suggested in Refs. [4,5]. However, the band filling obtained by our calculation does not agree with that obtained from the extended Hückel semiempirical calculations. One gets about $2/3$ of electron associated to each chain, against 0.82 electron for chain a and 0.59 electron for chains $a \pm b$ in Ref. [5].

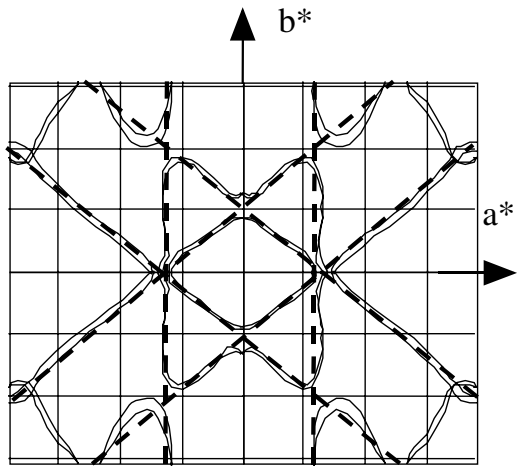

FIG. 3. DFT calculated FS in the $c^* = 0$ reciprocal plane of $P_4W_8O_{32}$. Dotted lines are superimposed on the calculated FS in order to show that the surface can be decomposed into the sum of three independent quasi-1D FS's.

To calculate the electron-hole response function of the system, we have used formula (1) for which the occupation numbers were taken using the Fermi-Dirac distribution at 100 K. The response function calculated in the a^*b^* reciprocal plane is shown in Fig. 1C. The maxima of $\chi(q, T)$ form two sets of broad lines perpendicular to the $a \pm b$ directions. Weaker maxima form faint lines perpendicular to the a direction. The maxima of $\chi(q, T)$ are exactly located at the position of the diffuse lines revealed by the x-ray diffuse scattering investigation (see Fig. 1A). This agreement unambiguously proves that the CDW instability of $P_4W_8O_{32}$ is triggered by the divergence of the electron-hole response function. More quantitatively the inverse of the half width at maximum of the lines of maxima of $\chi(q, T)$ leads to a CDW thermal coherence length at $T = 300$ K of

$$\xi_a = \frac{\hbar v_F}{\sqrt{2}\,\pi kT} = 1.4 \pm 0.2 \text{ nm};$$

$$\xi_{a+b} = 0.6 \pm 0.2 \text{ nm},$$

where v_F is the Fermi velocity. These values are in very good agreement with the intrachain correlation lengths deduced from the diffuse scattering experiments [15].

As shown in Fig. 1C, the strongest values of $\chi(q, T)$ are located at the crossing points of all the diffuse lines. The first maximum is located at $(0.34, 0)$ in the (a^*, b^*) plane, which is precisely the components of the q_2 critical CDW wave vector. The four other maxima are located at $(0, 0.35)$, the Brillouin zone boundaries, and at $(0.33, 0.31)$ which is close to the q_1 critical CDW wave vector. Thus, the wave vectors which maximize the electronic response function correspond to the critical wave vectors involved in the successive CDW transitions. However, experimentally, the high temperature q_1 modulation does not correspond to the strongest maximum of $\chi(q, T)$. Though we clearly demonstrate a correlation between the maxima in the DFT Lindhard response function and the experimental transition wave vectors, we are not able to relate the intensities of the divergences to the transition temperatures. However, when studying the CDW transitions considering only the eigenenergies of the Kohn-Sham equations [20] for the high temperature structure [ϵ_k in formula (1)], one

cannot expect to predict how the total energy (internal energy) varies when the phase is modulated. Consequently, and in order to compare the stability of the different modulated phases and to conclude more quantitatively about the DFT expected transition temperatures, one would need to estimate the changes in the total energies (enthalpies) considering all kinds of modulations. Because the potential energy surface is highly anharmonic and has many dimensions (the high temperature unit cell contains 44 atoms, the low temperature structures are incommensurate), even a rough study would be computationally very difficult. Nevertheless, the fact that DFT predicts good transition wave vectors proves the relevance of the standard Peierls scenario to explain the CDW transitions in $P_4W_8O_{32}$.

The hypothesis which considers the global FS of the ReO_3-type layered transition metal oxide bronze as the superposition of the FS of three different independent chains has been confirmed by self-consistent DFT calculations of the FS of $P_4W_8O_{32}$. The calculation of the electron-hole Lindhard response function based on this FS quantitatively accounts for the experimental determination of the wave vector dependence of the CDW fluctuations. This proves that the hidden nesting mechanism is at the origin of the CDW instability of the transition metal oxides. These findings can be relevant for the general field of the 2D oxides where there is now more and more evidence that 1D-like anisotropic physical phenomena are present.

We thank E. Canadell, J. Dumas, H. Guyot, and C. Schlenker for useful discussions. We also acknowledge M. Greenblatt, D. Groult, and P. Labbé for their collaboration concerning the synthesis of the samples.

[1] Special issue on Common Trends in Synthetic Metals and High-T_c Superconductors [J. Phys. I (France) **6** (1996)].
[2] Special issue on Oxide Bronzes, edited by M. Greenblatt [Int. J. Mod. Phys. B **23–24** (1993)].
[3] *Physics and Chemistry of Low-Dimensional Inorganic Conductors,* edited by C. Schlenker *et al.,* NATO ASI, Ser. B, Vol. 354 (Plenum Press, New York, 1996).
[4] M.-H. Whangbo, E. Canadell, P. Foury, and J.-P. Pouget, Science **252**, 96 (1991).
[5] E. Canadell and M.-H. Whangbo, in Ref. [2], p. 4005; in Ref. [3], p. 271.
[6] K. Breuer *et al.,* Phys. Rev. Lett. **76**, 3172 (1996).
[7] H. Guyot (private communication).
[8] P. Foury and J.-P. Pouget, in Ref. [2], p. 3973.
[9] C. Schlenker *et al.,* in Ref. [1], p. 2061; in Ref. [3], p. 115.
[10] C. Hess *et al.,* Physica (Amsterdam) **282C–287C**, 955 (1997).
[11] M. Sasaki *et al.,* Synth. Met. **103**, 2660 (1999).
[12] J. P. Giroult *et al.,* Acta Crystallogr. Sect. B **37**, 2139 (1981).
[13] M. Greenblatt, in Ref. [2], p. 3937; in Ref. [3], p. 15.
[14] J. Lüdecke, A. Jobst, and S. van Smaalen, Europhys. Lett. **49**, 357 (2000).
[15] The correlation lengths, inversely proportional to the half width at half maximum of the diffuse sheet, are 1.2 ± 0.3 nm along the a chain and 0.8 ± 0.3 nm along the $a \pm b$ chains, at room temperature (Fig. 1A).
[16] J.-P. Pouget, in Ref. [3], p. 185.
[17] X-ray diffuse scattering experiments measure the $\chi_\rho(q,T)$ response. In the random phase approximation of the electron-phonon coupling λ_q (valid at high temperature), $\chi_\rho(q,T) = \frac{\chi(q,T)}{1-\lambda_q\chi(q,T)}$. However, $\chi_\rho(q,T)$ has the anisotropy of $\chi(q,T)$ when, as usual, λ_q has a smooth dependence with q.
[18] G. Grüner, *Density Waves in Solids,* Frontiers in Physics Vol. 89 (Addison-Wesley, Reading, MA, 1994).
[19] This response function is given for free electrons where the matrix elements between Bloch states are equal to unity.
[20] M. C. Payne *et al.,* Rev. Mod. Phys. **64**, 1046 (1992).
[21] R. W. Nunes and D. Vanderbilt, Phys. Rev. B **50**, 12 025 (1994).
[22] G. Kresse and J. Furthmuller, Phys. Rev. B **54**, 17 611 (1996).
[23] Neglecting the energy dependence of the relaxation time, the thermopower of a 1D metal is given by $S = -(\pi^2 k_B T/6e)\cos 2\pi k_F/E_F \cos^2 \pi k_F$. Using the experimental value $dS/dT = -30$ nV/K^2 and with $2k_F = 1/3$, one gets $E_F \approx 0.3$ eV for the $m = 4$ member [see C. Hess *et al.,* Synth. Met. **86**, 2189 (1997)].
[24] L. Roca, A. Mascaraque, M. C. Ascencio, S. Drouard, and H. Guyot (private communication).
[25] E. Canadell and M.-H. Whangbo, Chem. Rev. **91**, 965 (1991).
[26] For the two conduction bands of the blue bronze $K_{0.3}MoO_3$, the photoemission measurements give $E_F^1 = 0.4$ eV, $E_F^2 = 1.4$ eV to be compared with $\check{E}_F^1 = 0.18$ eV, $\check{E}_F^2 = 0.3$ eV calculated by the extended Hückel method [G.-H. Gweon *et al.,* J. Phys. Condens. Matter **8**, 9923 (1996)].